

Cannabinoid receptor 2 deficiency results in reduced neuroinflammation in an Alzheimer's disease mouse model



Anne-Caroline Schmöle^{a,b}, Ramona Lundt^a, Svenja Ternes^a, Önder Albayram^a,
Thomas Ulas^c, Joachim L. Schultze^c, Daniele Bano^b, Pierluigi Nicotera^b,
Judith Alferink^{a,d,e}, Andreas Zimmer^{a,*}

^a Institute of Molecular Psychiatry, University of Bonn, Bonn, Germany

^b German Center for Neurodegenerative Diseases (DZNE), Bonn, Germany

^c Life and Medical Sciences (LIMES) Institute, Genomics and Immunoregulation, University of Bonn, Germany

^d Department of Psychiatry, University Münster, Münster, Germany

^e Cluster of Excellence EXC 1003, Cells in Motion, Münster, Germany

ARTICLE INFO

Article history:

Received 11 April 2014

Received in revised form

1 September 2014

Accepted 17 September 2014

Available online 28 September 2014

Keywords:

Alzheimer's disease

CB2

CCL2

Endocannabinoid system

Microglia

Neuroinflammation

ABSTRACT

Several studies have indicated that the cannabinoid receptor 2 (CB2) plays an important role in neuroinflammation associated with Alzheimer's disease (AD) progression. The present study examined the role of CB2 in microglia activation in vitro as well as characterizing the neuroinflammatory process in a transgenic mouse model of AD (APP/PS1 mice). We demonstrate that microglia harvested from CB2^{-/-} mice were less responsive to pro-inflammatory stimuli than CB2^{+/+} microglia, based on the cell surface expression of ICAM and CD40 and the release of chemokines and cytokines CCL2, IL-6, and TNF α . Transgenic APP/PS1 mice lacking CB2 showed reduced percentages of microglia and infiltrating macrophages. Furthermore, they showed lowered expression levels of pro-inflammatory chemokines and cytokines in the brain, as well as diminished concentrations of soluble A β 40/42. The reduction in neuroinflammation did not affect spatial learning and memory in APP/PS1*CB2^{-/-} mice. These data suggest a role for the CB2 in Alzheimer's disease-associated neuroinflammation, independent of influencing A β -mediated pathology and cognitive impairment.

© 2015 Elsevier Inc. All rights reserved.

1. Introduction

Alzheimer's disease (AD) is a neurodegenerative disorder and represents the most common type of dementia among the elderly population. Neuropathological hallmarks characteristic of AD include amyloid- β (A β) plaques and neurofibrillary tangles, accompanied by neuroinflammation characterized by astrocytosis and microgliosis. Microglia attracted to A β deposits represent the primary cellular component associated with AD neuroinflammation. In response to immune-stimulatory signals, they change from a resting to an activated state. Activated microglia express at least 2 phenotypes depending on their environmental stimulation: an M(IFN γ), formerly known as M1, phenotype associated with the production of proinflammatory mediators and an M(IL-4), formerly known as M2, alternatively activated phenotype characterized by anti-inflammatory qualities (Michelucci et al.,

2009; Murray et al., 2014). Several studies have shown that A β -mediated activation of microglia induces the production of various chemokines and cytokines, neurotoxic secretory products, free radical species, and NO intermediates (Heneka, et al., 2010). These proinflammatory mediators cause neuronal dysfunction and cell death, suggesting that activation of microglia plays a prominent role in neuroinflammation in the context of AD. In addition to activation of the pro-inflammatory cascade, microglia cells have also been shown to phagocytize A β plaques, thereby reducing the number of protein aggregates in an AD brain (Bolmont et al., 2008).

The endocannabinoid system (ECS) is a retrograde messenger system consisting of lipid signaling molecules that bind to at least 2 G-protein-coupled receptors. Cannabinoid receptor 1 (CB1) is mainly expressed in the central nervous system (CNS) but has also been detected in lung, kidney, and liver. In contrast, CB2 is primarily expressed on immune cells such as B-cells, T-cells, macrophages, dendritic cells, and microglia (Pacher and Mechoulam, 2011). Thus, the ECS affects both immune responses and cognition. In addition, studies have suggested that CB2 plays a role in the modulation of microglia activity relevant to AD.

A.-C.S. and R.L. contributed equally and J.A. and A.Z. shared senior authorship.

* Corresponding author at: Institute for Molecular Psychiatry, University of Bonn, Sigmund-Freud-Strasse 25, 53127 Bonn, Germany. Tel.: +49 (0)228 6885 300; fax: +49 (0)228 6885 301.

E-mail address: a.zimmer@uni-bonn.de (A. Zimmer).

Early studies already suggested a crucial role for the CB2 receptor in AD, based on findings that CB2 is overexpressed in A β plaque-associated microglia (Benito et al., 2003). Up-regulation of CB2 expression by microglia has also been described in Huntington disease, simian immunodeficiency virus-induced encephalitis, human immunodeficiency virus (HIV) encephalitis, and multiple sclerosis (Benito et al., 2003, 2005, 2008; Ramírez et al., 2005).

To date however, most studies have examined the effects of pharmacological modulation of the ECS, showing that stimulation with specific CB2 agonists reduces the A β burden and neuroinflammation and rescues cognitive deficits in AD mouse models (Aso et al., 2013). Similar observations were also made in rats injected with amyloid fibrils in the hippocampal CA1 region to mimic AD pathology, followed by treatment with a CB2 agonist (Wu et al., 2013). In addition, extended oral treatment with cannabinoids reduced A β levels of APP2576 mice (Martín-Moreno et al., 2012) and decreased A β plaque-deposition in 5xFAD APP transgenic mice (Chen et al., 2013). However, since the precise involvement of cannabinoid receptors remains unknown, we investigated here CB2 in AD using *in vitro* and *in vivo* models. Our results indicate an important function of CB2 in the modulation of AD-associated neuroinflammation.

2. Methods

2.1. Microglia cultures

Primary neonatal microglia were generated from 1- to 5-day-old C57BL/6J (CB2^{+/+}) and CB2^{-/-} pups (Buckley et al., 2000), according to the protocol from Saura et al. (Saura et al., 2003). Briefly, after cervical dislocation, extracted brains were collected in ice-cold phosphate-buffered saline (PBS). Cortices of both hemispheres were collected after removal of meninges and triturated until a single-cell suspension was achieved. Isolated cells were cultivated as mixed glia culture until they reached confluency at approximately 21 days. Cells were cultivated in Dulbecco's modified Eagle's medium (DMEM) high-glucose (Gibco, Darmstadt, Germany) containing 10% fetal calf serum (FCS) (PAA, Freiburg, Germany), 1% penicillin/streptomycin (Gibco), 1% MEM/NEAA (Gibco), and 0.001% β -mercaptoethanol (Gibco), medium was changed twice weekly. Microglia cells were harvested by mild trypsinization and re-seeded in 24-well-plates for stimulation experiments or phagocytosis assay at a density of 1.5×10^5 cells/mL. After re-seeding, cells rested for 24 hours.

For stimulation, cells were treated for 16 hours with LPS (100 ng/mL) (Sigma-Aldrich, Taufkirchen, Germany) and interferon- γ (IFN γ ; 20 ng/mL) (R&D Systems, Wiesbaden, Germany) or for 48 hours with interleukin-4 (IL-4; 100 U/mL) (eBioscience, Frankfurt, Germany).

2.2. Phagocytosis assay

Microglia cells were incubated with fluorescently labeled A β 42 (Alexa-Flour 649) for 1 hour at room temperature, or at 4 °C as a negative control for unspecific binding. Labeling of A β was performed by using DyLightTM649 Microscale Antibody Labeling Kit (ThermoScientific, Waltham, MA). After washing, cells were stained with CD11b antibodies for flow cytometry.

2.3. Animals

APP/PS1 mice were purchased from Charles River Laboratories (B6.Cg-Tg (APP^{swe}(K594 N/M595 L)/PSEN1dE9)85Dbo/J; Charles River Laboratories, Germany GmbH) and crossed with CB2^{-/-} mice (Buckley et al., 2000). APP/PS1*CB2^{+/-} mice were then crossed with

CB2^{-/-} mice. All animals were bred and housed in a specific pathogen-free animal facility under standard animal housing conditions in a 12h dark-light cycle with access to food and water *ad libitum* according to German guidelines for animal care. APP/PS1*CB2^{-/-} pups were born at a less-than-expected ratio. We thus crossed APP/PS1*CB2^{-/-} mice with CB2^{-/-} mice. The experiments were carried out with mice at the age of 9 and 14 months from both breeding strategies. Mice were genotyped by polymerase chain reaction (PCR) using DNA from tail tissue. Primers: CB2 common (5'-GTC GAC TCC AAC GCT ATC TTC-3'), CB2 wild-type (5'-GTG CTG GGC AGC AGA GCG AAT C-3'), CB2 knock-out (5'-AGC GCA TGC AGA CTG CCT-3'), PSEN1-F (5'-GGT CCA CTT CGT ATG CTG-3'), and PSEN-R (5'-AAA CAA GCC CAA AGG TGA T-3').

Experimental procedures complied with all regulations for animal experimentation in Germany and were approved by the Landesamt für Natur, Umwelt und Verbraucherschutz in Nordrhein-Westfalen, Germany (AZ 87-51.04.2011.A041, 8.84-02.05.20.11.101).

2.4. Isolation of intracerebral mononuclear cells

Brains were removed after intracardial perfusion with ice-cold PBS and minced with small scissors followed by trituration with a 20-gauge needle. Brain fragments were incubated with 1 mL collagenase solution (Roche, Mannheim, Germany) (1 mg/mL) for 45 minutes at 37 °C. Subsequently, tissue fragments were triturated with 1 mL DNase solution (Roche) (1 mg/mL) and incubated for 45 minutes at 37 °C. After establishing a single-cell suspension, cells were washed and re-suspended in 70% percoll solution (GE Healthcare, Uppsala, Sweden) and overlaid with a 30% percoll solution before spinning down for 25 minutes without a break. Mononuclear cells were collected at the interphase, washed with PBS, and, after centrifugation at 1800 rpm for 10 minutes at 4 °C, subjected to cell surface marker staining for flow cytometry.

2.5. Flow cytometry

Cells were labeled with fluorochrome-coupled anti-mouse antibodies or biotin-coupled anti-mouse antibodies, followed by incubation with streptavidin-fluorochrome coupled secondary reagents. Antibodies (RRID): CD11 b (AB_469343), CD11 b (AB_394773), CD11 b (AB_1582236), CD11 b (AB_312789), CD11 b (AB_465549), CD40 (AB_465651), CD16/32 (AB_312801), MMR (CD206) (AB_2144899), ICAM (CD54) (AB_465095). Immunofluorescence of labeled cells was subsequently measured by using a FACS Canto II (BD Bioscience, Heidelberg, Germany), equipped with FACSDiva software. Data analysis was performed using FlowJo software (Tree Star Inc, Ashland, OR).

2.6. Total RNA preparation

RNA was extracted by TRIzol extraction protocol. Briefly, frozen tissue was homogenized in 1 mL or 800 μ L TRIzol (Invitrogen, Camarillo, CA). After precipitation with isopropanol, RNA was stored at -80 °C. For cDNA synthesis, 400 ng RNA was incubated for 5 minutes at 65 °C and then reverse transcribed at 42 °C for 50 minutes. A total volume of 20 μ L included 4 μ L first-strand buffer (Invitrogen), 2 μ L 0.1 mo/L DTT, 1 μ L 10 mmol/L dNTPs, 1 μ L oligo(dT)20 primer (Invitrogen), and 200 U SuperScript II reverse transcriptase (Invitrogen).

2.7. Quantitative RT-PCR

RT-quantitative PCR of cDNA samples was performed using ABI 7900 sequence detector (Perkin-Elmer, Waltham, MA) and

Universal PCR Master Mix (Perkin-Elmer). A 25 ng quantity of cDNA was used per reaction. Standard program were applied as follows: step 1 (1x) 95 °C, 10 minutes; step 2 (40x) 95 °C, 15 seconds and 60 °C, 1 minute. TaqMan primer (all Applied Biosystems, Foster City, CA): *il-6* (Mm0446190_m1), *il-10* (Mm99999012_m1), *tnf* (Mm00443258_m1), *ccl2* (Mm00441242_m1), *arg1* (Mm00475988_m1), *gapdh* (Mm9999915_g1).

2.8. RNA isolation for microarray

RNA was isolated from cells lysed in Qiazol using the miRNeasy Mini Kit (Qiagen) according to the manufactures' protocol. The precipitated RNA was solved in RNase free water. The quality of the RNA was assessed by measuring the ratio of absorbance at 260 nm and 280 nm using a Nanodrop 1000 Spectrometer (Peqlab) as well as by visualization of the integrity of the 28S and 18S band on a 1.2% agarose gel.

2.9. Gene expression profiling by Illumina Beadchip arrays and primary data handling

Biotin-labeled cRNA was generated using the TargetAmp Nano-g Biotin-aRNA Labeling Kit for the Illumina System (Epicentre). Biotin-labeled cRNA (1.5 µg) was hybridized to MouseWG-6 v2 Beadchips (Illumina) and scanned on an Illumina HiScanSQ system. Raw intensity data were processed in Genome Studio (Illumina), excluding probe sets with missing bead types to increase validity.

2.10. Data generation and bioinformatics of microarray data

Processing of raw-intensity data was performed by BeadStudio 3.1.1.0 (Illumina). Data were exported using the Partek report builder plugin and imported as non-normalized data into Partek Genomics Suite V6.6 (PGS). A total of 12 samples were imported into Partek Genomics Suite (PGS) and were then normalized using quantile normalization before further analysis. Batch effects of separate array experiments were removed from normalized log₂-transformed data. Differentially expressed (DE) genes between the different conditions, as well as transcripts with variable expression within the dataset, were calculated using 2-way analysis of variance (ANOVA) models including batch correction. DE genes were defined by a fold change (FC) greater than 2, and a false discovery rate (FDR)-corrected *p* value of < 0.05 unless stated otherwise. Microglia microarray data are accessible via super-series GSE60903.

2.11. Aβ soluble quantification: Enzyme-linked immunosorbent assay

Aβ 40 (Invitrogen KHB381) and Aβ 42 (Invitrogen KHB3441) enzyme-linked immunosorbent assays (ELISAs) were conducted according to the manufacturer's protocol. Briefly, precoated wells were incubated with Aβ peptide standards, controls, and samples with the addition of Aβ 40/Aβ 42 detection antibody for 3 hours at room temperature. After washing, IgG horseradish peroxidase working solution was added, and wells were incubated for 30 minutes. Plates were washed again, and stabilized chromogen was added and incubated for 30 minutes in the dark. Finally, stop solution was added, and absorbance was measured at 450 nm.

2.12. Immunohistochemistry

Sagittal brain slices of 12-µm thickness were stained with primary antibodies anti-mouse Iba1 (rabbit) diluted 1:500 over night at 4 °C. Incubation with secondary antibody goat anti-rabbit

coupled to Cy3 fluorochrome for 1 hour at room temperature, followed by counterstaining with DAPI. Antibodies: Iba1 (AB_10641962), GFAP (AB_305808), Goat-anti-rabbit Cy3 (AB_10563288). For plaque analysis, slices were incubated with 0.025 % (w/v) thioflavin S solution (1:2 EtOH/PBS) for 1 minute. Pictures were taken with an inverse fluorescence microscope (10×/20×) (Zeiss Axiovert 40 CFL, AxioCamMRm).

2.13. Morris Water Maze

Spatial learning and memory of mice was analyzed by the Morris Water Maze (MWM) test with 5 consecutive training days, each day with 4 training trials in which escape latency to the hidden platform was measured. On the sixth day, a probe trial was performed, in which the platform was removed and time spent in each quadrant was measured. Three different cohorts of mice were tested, 1 cohort at the age of 6 months, 1 at the age 9 months, and 1 at the age of 14 months.

2.14. Cytokine quantification

The murine IL-6, tumor necrosis factor-α (TNFα) and CCL2 Ready-SET-Go! ELISA kits (eBioscience) were used to quantify the levels of these cytokines and chemokines in cell culture supernatants. Quantitative determination was carried out according to manufacturer's protocol.

2.15. Statistical analysis

Statistical analysis was performed using 2-way analysis of variances (ANOVA), followed by Fisher post hoc test if appropriate (version 6.0 d, Prism software, GraphPad, San Diego, CA). A value of *p* < 0.05 was considered to be significant.

3. Results

3.1. Primary CB2^{-/-} microglia exhibit decreased responses to pro-inflammatory stimuli

To assess the functional role of CB2 in the inflammatory response, we first investigated if primary CB2^{+/+} microglia express the CB2 receptor and other components of the ECS, such as DAGL, MAGL, or FAAH. Thus, we stimulated primary microglia derived from 1- to 5-day-old CB2^{+/+} mice with either a pro- or anti-inflammatory stimulus and evaluated CB2 receptor expression by microarray. CB2^{+/+} microglia express the CB2 receptor under control conditions. IL-4 stimulation did not alter CB2 expression compared to control conditions, but stimulation with lipopolysaccharide (LPS) and interferon-γ (IFNγ) led to a significant decrease in CB2 expression (Table 1). Both LPS/IFNγ as well as IL-4 stimulation were able to modify expression of components of the ECS. Next, we stimulated primary microglia derived from CB2^{-/-} mice with LPS/IFNγ and compared their cell surface marker expression profile with CB2^{+/+} cells or unstimulated controls. CB2^{-/-} microglia showed a reduced expression of the pro-inflammatory cell surface marker intercellular adhesion molecule-1 (ICAM-1), at baseline as well as lower responses to LPS/IFNγ stimulation than CB2^{+/+} cells (Fig. 1A). Although CB2^{+/+} and CB2^{-/-} microglia both showed a significant upregulation of ICAM-1 expression after LPS/IFNγ stimulation (2-way ANOVA, followed by Fisher post hoc test; *p* < 0.001), there was a significant genotype effect at baseline and after stimulatory conditions (*p* < 0.001 and *p* < 0.01). CD40 expression was similar to that of ICAM-1 in that its expression levels were significantly reduced in CB2^{-/-} microglia compared to CB2^{+/+} microglia after stimulation with LPS/IFNγ (Fig. 1B) (*p* < 0.001; *n* = 2,

Table 1

Expression of endocannabinoid system (ECS) components in stimulated neonatal microglia

Gene	LPS/IFN γ		IL4	
Cnr1	1.08008	↑**	0.99435	↓
Cnr2	0.36891	↓***	1.30106	↑
Dagl α	1.05582	↑	1.03996	↑
Dagl β	0.77895	↓*	1.01716	↑
Napepld	1.58681	↑	1.40618	↑
Faah	1.23968	↑	1.07403	↑
Mgll	1.18301	↑	1.30390	↑*
Abhd6	1.13530	↑	1.03518	↑
Abhd12	0.21966	↓*	1.05757	↑

Expression of ECS components in CB2^{+/+} microglia in the presence of LPS/IFN γ or IL4. Data are presented as fold-change compared to nonstimulated cells. Stimulus-dependent regulations were detected for Napepld, Dagl β , Cnr2, and Abhd12. Data were analyzed by 2-way analysis of variance with FDR based on Benjamini Hochberg, *p < 0.05, **p < 0.001, ***p < 0.005 to unstimulated control.

Key: Abhd6, A β -hydrolase 6; Abhd12, hydrolase 12; Cnr1, cannabinoid receptor 1; Cnr2, cannabinoid receptor 2; Dagl α/β , diacylglycerol lipase α/β ; Faah, fatty-acid-amide hydrolase; IFN, interferon; IL, interleukin; LPS, lipopolysaccharide; Mgll, monoacylglycerol lipase; Napepld, N-arachidonoyl-phosphatidylethanolamine phospholipase D.

all samples were analyzed in triplicate). However, baseline levels were not statistically different.

We further analyzed the release of cytokines and chemokines as markers of microglial activation. Stimulation of neonatal microglia

with LPS/IFN γ led to an increased secretion of IL-6 and TNF α in both CB2^{+/+} and CB2^{-/-} microglia (Fig. 1C and D). However, we observed a significantly lower production of these cytokines in stimulated CB2^{-/-} cells (p < 0.001 in IL-6 and TNF α). The genotype difference was even more pronounced for CCL2 secretion (p < 0.001), which was strongly induced by LPS/IFN γ in CB2^{+/+} microglia, but remained constant in cells from CB2^{-/-} mice after LPS/IFN γ stimulation (Fig. 1E).

3.2. CB2 deficiency in neonatal microglia does not affect phagocytosis of A β

Because cell surface marker and cytokine expression profiles differed between CB2^{+/+} and CB2^{-/-} neonatal microglia after challenge with LPS/IFN γ , we next determined whether the reduced pro-inflammatory activation profile observed in CB2^{-/-} microglial cells was associated with changes in phagocytosis efficiency by measuring the uptake of fluorescently labeled A β by neonatal CB2^{+/+} and CB2^{-/-} microglia using flow cytometry. Similar levels of A β 42-DyLight649 uptake were observed between CB2^{+/+} and CB2^{-/-} neonatal microglia, demonstrating that the presence or absence of CB2 did not affect the efficiency of A β phagocytosis (Fig. 2A and B).

3.3. CB2 deficiency leads to decreased microgliosis and macrophage invasion in APP/PS1 mice

To investigate the role of CB2 in the neuroinflammatory process associated with Alzheimer's disease, we crossed transgenic APP_{swe}/PSEN1 Δ E9 (APP/PS1) mice with CB2^{-/-} mice. APP/PS1 mice develop high plaque loads associated with enhanced neuroinflammatory responses, accelerated deficits in memory

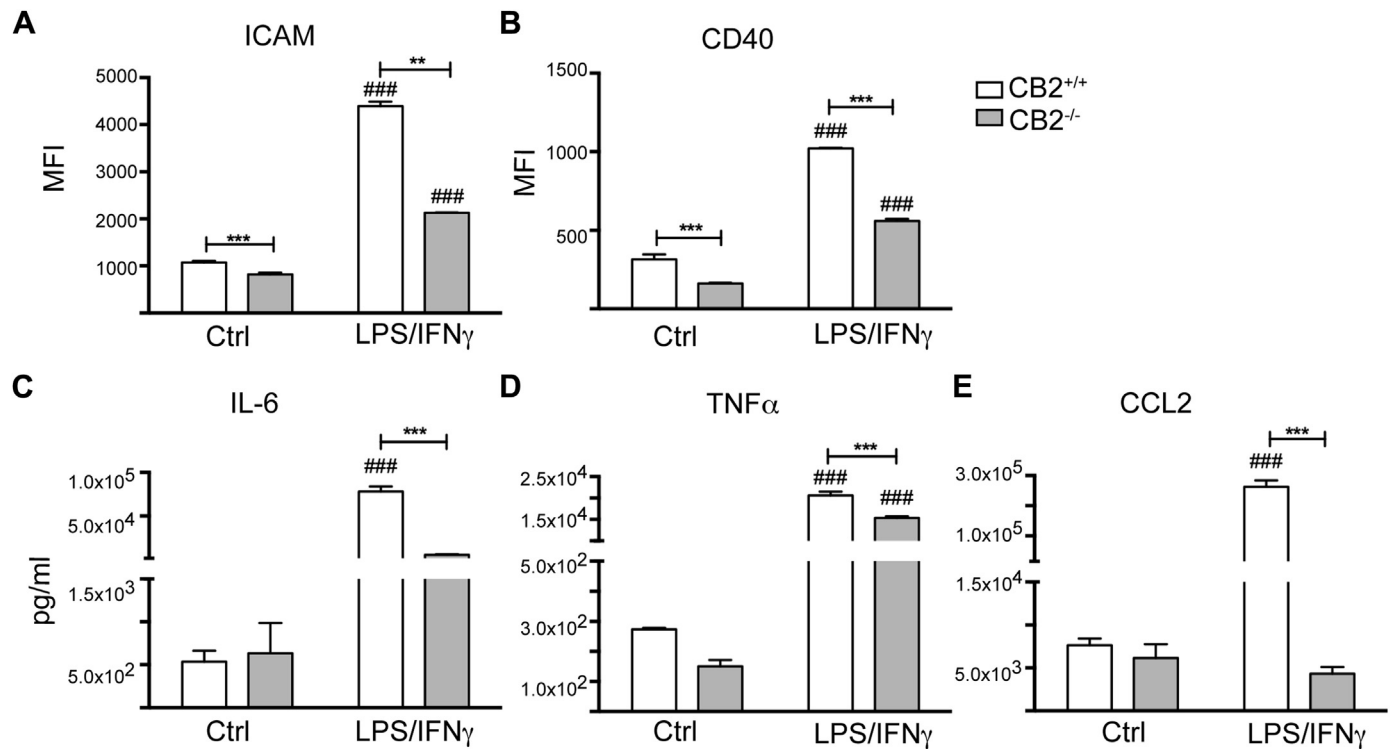


Fig. 1. Expression of cell surface markers and release of pro-inflammatory chemokines and cytokines by stimulated neonatal microglia from CB2^{+/+} and CB2^{-/-} mice. Expression of ICAM-1 (A) and CD40 (B). CB2^{-/-} microglia show a reduced surface expression of ICAM-1 and CD40 compared to CB2^{+/+} microglia (A and B). N = 3, all samples were analyzed in triplicates. Data shown in Fig. 1 C, D, and E are representative for 1 of 3 experiments. Release of IL-6 (C), TNF α (D), and CCL2 (E), CB2^{-/-} microglia show a different expression pattern compared to CB2^{+/+} microglia. N = 2; all samples were analyzed in triplicate. Data were analyzed by 2-way analysis of variance, followed by Fisher post hoc test, *p < 0.05, **p < 0.001, ***p < 0.005 to CB2^{+/+}, #significance to unstimulated genotype control.

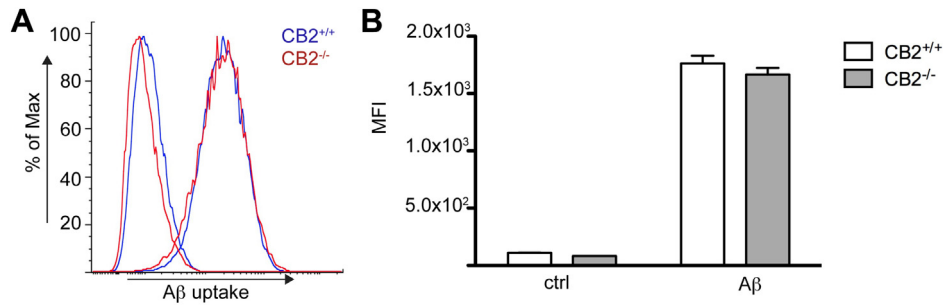


Fig. 2. Phagocytosis of A β in CB2^{+/+} and CB2^{-/-} neonatal microglia. Uptake of A β was determined by flow cytometry (A and B). Phagocytosis of A β by CB2^{-/-} microglia is equivalent to CB2^{+/+} cells. N = 2; all samples were analyzed in triplicate. Data shown in Fig. 2 are representative for 1 of 2 experiments. Data were analyzed by 2-way analysis of variance, followed by Fisher post hoc test. (For interpretation of the references to color in this Figure, the reader is referred to the web version of this article.)

and learning (Lee et al., 1997), and cognitive deficits starting at the age of 9 months (Gordon et al., 2001). We first investigated if microgliosis was affected by the absence of CB2 signaling in APP/PS1 mice by staining sagittal brain slices of 14-month-old

mice with anti-Iba1 (Fig. 3A). This analysis demonstrated enhanced immunoreactivity of Iba1 in the brains of APP/PS1 mice compared to wild-type (WT) controls (2-way ANOVA, followed by Fisher post hoc test, $p < 0.001$), indicative of enhanced

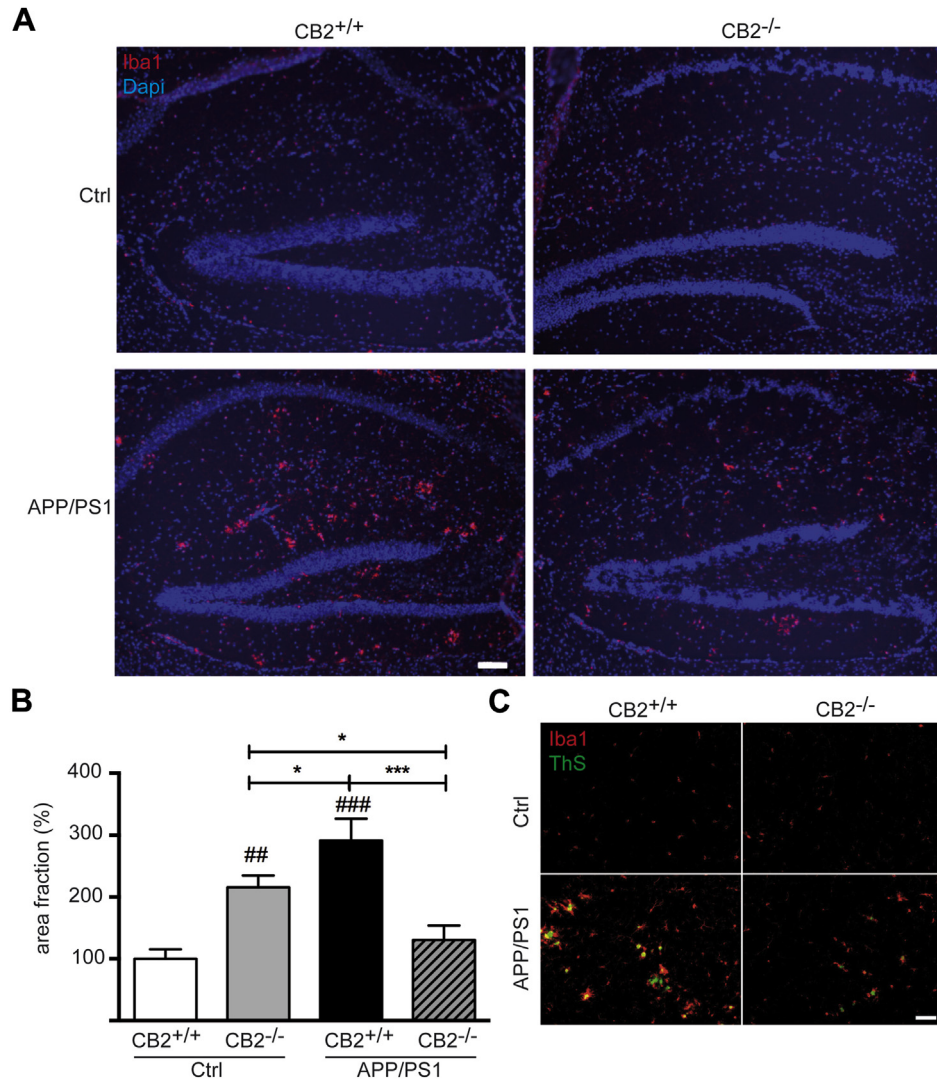


Fig. 3. Analysis of CB2-dependent microgliosis in aged APP/PS1*CB2^{-/-} mice. Immunofluorescence analysis of Iba1 expression in the hippocampus of APP/PS1*CB2^{-/-} mice. Shown are representative brain tissue sections stained for Iba1 (red) and counterstained with DAPI (blue) of CB2^{+/+}, CB2^{-/-}, APP/PS1, and APP/PS1*CB2^{-/-} mice at the 14 months (A). Microgliosis is significantly enhanced in APP/PS1 mice compared to CB2^{+/+} mice (scale bar = 100 μ m). In contrast, APP/PS1*CB2^{-/-} mice show significantly reduced microgliosis compared to APP/PS1 mice. N = 3 or 4; data were analyzed by 2-way analysis of variance, followed by Fisher post hoc test, * $p < 0.05$, ** $p < 0.01$, *** $p < 0.001$, #significance to wild-type control (B). APP/PS1 and APP/PS1*CB2^{-/-} mice show co-localization of Iba1-positive microglia with Thioflavin-stained A β plaques (scale bar = 50 μ m) (C). (For interpretation of the references to color in this Figure, the reader is referred to the web version of this article.)

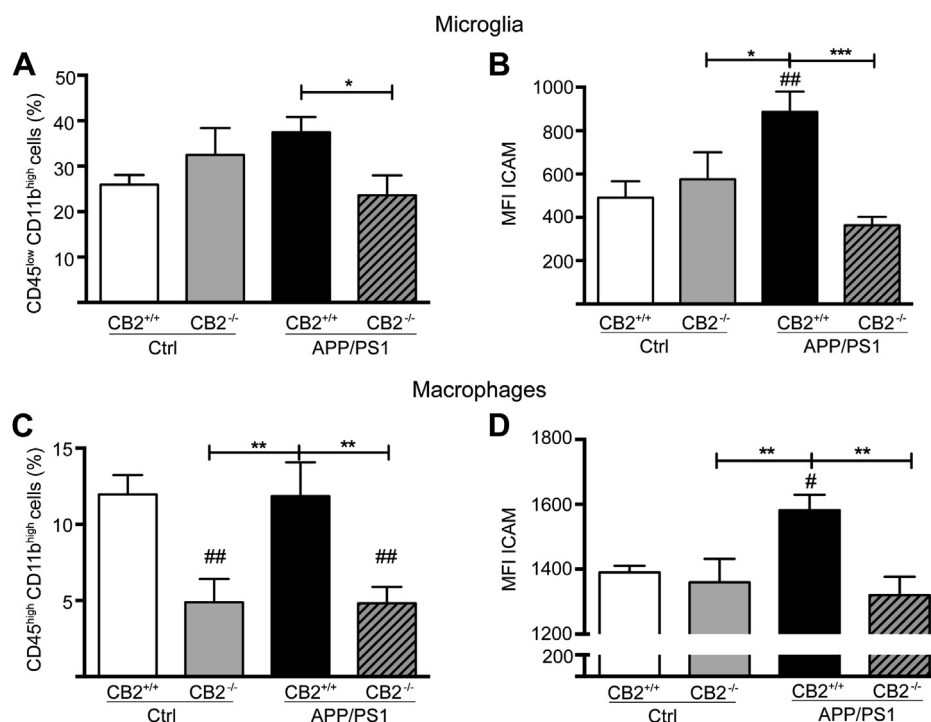


Fig. 4. Analysis of intracerebral mononuclear cells in the brains of aged APP/PS1 mice. Flow cytometry of intracerebral mononuclear cells of 14-month-old mice. Microglia cells were determined as CD11b^{pos}/CD45^{low}, infiltrating macrophages as CD11b^{pos}/CD45^{high}. APP/PS1 mice show enhanced microgliosis (A). Both, CB2^{-/-} and APP/PS1*CB2^{-/-} have a significantly reduced number of macrophages compared to CB2^{+/+} and APP/PS1 mice (C). Enhanced ICAM expression levels in microglia and brain macrophages of APP/PS1 mice (B and D). N = 6; data were analyzed by 2-way analysis of variance, followed by Fisher post hoc test, * $p < 0.05$, ** $p < 0.01$, *** $p < 0.001$, #significance to wild-type control.

microgliosis. In contrast, APP/PS1 mice lacking CB2 showed baseline Iba1 immunoreactivity (Fig. 3B), even though Iba1-immunoreactivity was significantly increased in CB2^{-/-} mice compared to CB2^{+/+} mice ($p < 0.01$). Both APP/PS1 and APP/PS1*CB2^{-/-} show Iba1-positive cells co-localized with Thioflavin-S-positive A β -plaques (Fig. 3C).

We next performed flow cytometric analyses of brain cells harvested from 14-month-old APP/PS1 and APP/PS1*CB2^{-/-} mice to evaluate the percentages of microglial cells (CD45^{low}/CD11b^{high}) and brain-infiltrating macrophages (CD45^{high}/CD11b^{high}) compared to percentages in either CB2^{+/+} or CB2^{-/-} mouse brains (Fig. 4).

In line with the Iba1 staining pattern observed, APP/PS1*CB2^{-/-} mice displayed a reduced percentage ($p < 0.05$) of microglia cells compared to APP/PS1 mice (Fig. 4A). APP/PS1*CB2^{-/-} mice as well as CB2-deficient mice showed a significantly reduced brain macrophage infiltration ($p < 0.01$), based on the lower percentage of CD45^{high} CD11b⁺ cells detected compared to WT and APP/PS1 mice. Surprisingly, the percentage of invading macrophages was not altered in APP/PS1 mice compared to age-matched controls. These data clearly indicate that CB2 modulates macrophage migration into the CNS (Fig. 4C).

Expression of the cell surface marker ICAM-1 on both, microglia and infiltrating macrophages was strongly increased in APP/PS1*CB2^{+/+} mice ($p < 0.01$ in microglia and $p < 0.05$ in macrophages) compared to expression levels detected in CB2^{+/+} and CB2^{-/-} mice (Fig. 4B, D). In contrast, ICAM-1 expression levels in microglia and macrophages from APP/PS1*CB2^{-/-} mice was significantly reduced, indicating that CB2 plays a role in activating microglia and controlling macrophage infiltration of the CNS in APP/PS1 mice. These observations support the finding that CB2-deficient primary microglia displayed reduced ICAM-1 expression levels after stimulation with LPS/IFN γ in vitro.

3.4. TNF α and CCL2 expression levels are reduced in the brains of aged APP/PS1*CB2^{-/-} mice

Based on the observations that APP/PS1*CB2^{-/-} mice displayed a reduced number of infiltrating macrophages and microglia (which, in turn, showed lower expression levels of pro-inflammatory cell surface markers), we next characterized the expression profiles of TNF α , IL-6, CCL2, Arg-1, and IL-10 in the hippocampus of middle-aged (9-month-old) and aged (14-month-old) mice.

Middle-aged mice expressed TNF α , IL-6, CCL2, and Arg-1 (Fig. 5), but not IL-10 (data not shown). In 9-month-old mice, no genotype-dependent differences in the expression of TNF α , CCL2, and Arg-1 were detected. Only IL-6 levels were increased in CB2^{-/-} and APP/PS1*CB2^{-/-} mice compared to CB2^{+/+} and APP/PS1 controls, confirmed by a significant genotype effect of CB2 (2-way ANOVA, followed by Fisher post hoc test, ** $p < 0.05$ for CB2^{-/-} and * $p < 0.01$ for APP*CB2^{-/-}; Fig. 5A).

In 14-month-old mice, TNF α expression was significantly increased in the presence of the APP transgene compared to control mice; however this effect was reversed in the absence of CB2 (** $p < 0.01$; Fig. 5B). In addition, CCL2 expression was significantly decreased in the absence of CB2 (* $p < 0.05$; Fig. 5C). This supports our in vitro findings that demonstrated that neonatal CB2^{-/-} microglia cells secreted significantly less CCL2. In addition, Arg1 expression was not significantly altered in 9-month and 14-month old mice (Fig. 5D).

3.5. APP/PS1*CB2-deficient mice show reduced brain levels of soluble A β 40/42 but equivalent A β plaque load

To study the role of CB2 in amyloid pathology and to visualize A β plaques, we stained slices from brain hemispheres of 9- and

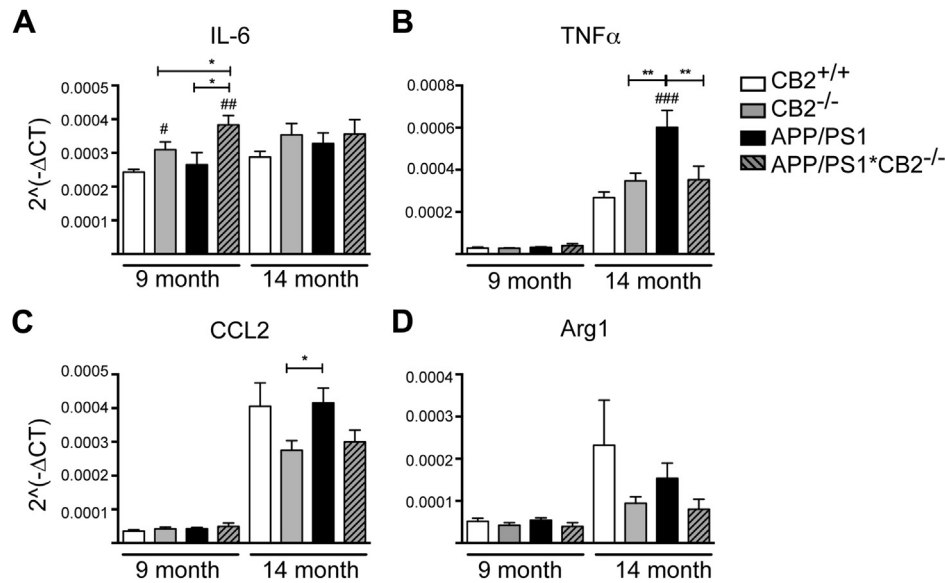


Fig. 5. Chemokine and cytokine expression in the hippocampus of aged APP/PS1 and control mice. Expression levels of IL-6, TNF α , CCL2, and Arg1 in the hippocampus of 9- and 14-month-old control, APP/PS1, and APP/PS1*CB2^{-/-} mice were analyzed by quantitative reverse transcription-polymerase chain reaction (RT-PCR). Nine-month-old mice show equivalent chemokine and cytokine expression of TNF α (B), CCL2 (C), and Arg1 (D). Only IL-6 levels were elevated in 9-month-old APP/PS1*CB2^{-/-} mice (A). In 14-month-old APP/PS1 mice increased TNF α secretion levels (B) were observed compared to control and APP/PS1*CB2^{-/-} mice (B). CCL2 expression in CB2 was dependently decreased compared to that in APP/PS1 and control mice. IL-6 and Arg1 expression did not differ in aged mice. N = 3 to 13; data were analyzed by 2-way analysis of variance, followed by Fisher post hoc test, * $p < 0.05$, ** $p < 0.01$, #significance to wild-type control.

14-month-old APP/PS1 and APP/PS1*CB2^{-/-} mice with Thioflavin-S to visualize A β plaques (Fig. 6A). The level of A β deposition in the hippocampus increased in an age-dependent manner in APP/PS1 mice regardless of CB2 expression (2-way ANOVA, followed by Fisher post hoc test, $p < 0.01$ and $p < 0.05$, respectively). APP/PS1*CB2^{-/-} mice showed a tendency toward decreased A β deposition compared to APP/PS1 mice, which was close to significance ($p = 0.0502$). Next, we measured the content of soluble A β 40 and 42 in brain homogenates of middle-aged and aged mice. At the age of 9 months, APP/PS1*CB2^{-/-} mice showed a lower content of A β 40 (Fig. 6C) and A β 42 (Fig. 6D) compared to APP/PS1 mice (Student t test, $p < 0.001$ and $p < 0.05$, respectively). However, at the age of 14 months, the levels were similar (Fig. 6E).

3.6. CB2 deficiency does not alter learning memory or performance in aged APP/PS1 mice

To determine whether CB2 deficiency influenced learning and memory in an AD mouse model, animals were tested using the Morris Water Maze. At the age of 6 months, we found a significant effect of the CB2 genotype on the acquisition of the task ($F_{1,85} = 4.609$, $p = 0.0113$). CB2^{-/-} animals showed significantly shorter escape latencies on days 2 and 3 compared to CB2^{+/+} (Fig. 7A). An even stronger CB2 genotype effect was observed in APP/PS1 transgenic animals ($F_{1,60} = 14.43$, $p < 0.0001$), as APP/PS1*CB2^{-/-} animals showed a significantly faster escape latency than APP/PS1*CB2^{+/+} mice at days 3 and 4 (Fig. 7B). This CB2 genotype effect was no longer present at the age of 9 or 14 months (Fig. 7C–F).

4. Discussion

In this study, we demonstrate that microglia harvested from CB2-deficient mice were less responsive to pro-inflammatory stimuli than microglia from control mice. In addition, CB2 deficiency in an AD mouse model leads to reduced microgliosis and macrophage invasion, associated with diminished expression of pro-inflammatory chemokines and cytokines. However, these

changes did not influence A β plaque load or learning and memory behavior at later stages of the disease.

Studies on brain tissues of AD patients have shown that A β -plaque-associated microglia express enhanced levels of CB2 (Benito et al., 2003), suggesting that CB2 modulates microglia function in the context of AD pathology. Furthermore pharmacological studies in rodents have also identified a crucial role for CB2 in AD-associated inflammatory processes (Wu et al., 2013), demonstrating that pharmacological activation of CB2 reduced microglia activation (Martín-Moreno et al., 2011, 2012) and had positive effects on cognition in AD animal models (Aso et al., 2013; Wu et al., 2013).

Interestingly, we demonstrated that CB2^{-/-} microglia cells expressed reduced levels of pro-inflammatory cell surface markers as well as a decreased response to stimulation with LPS/IFN γ . This was surprising based on observations by Ehrhart et al., which demonstrated that treatment of CB2^{+/+} primary microglia cells with the CB2 agonist JWH-015 also resulted in a reduced activation of microglia cells (Ehrhart et al., 2005), paradoxically showing that both genetic deletion and pharmacological activation of CB2 produced similar effects. Unfortunately, the effects of CB2 antagonists have not yet been investigated. It is possible that the general responsiveness to pro-inflammatory stimuli is altered in microglia with a genetic disruption of CB2. This should be clarified in future studies comparing the effects of CB2 agonists and antagonists.

Stimulation of neonatal microglia with LPS/IFN γ led to an increase in the secretion of TNF α and IL-6 in both CB2^{+/+} and CB2^{-/-} microglia, but the response observed in CB2^{-/-} microglia was less intense. Similarly, LPS-induced TNF α production was also reduced in microglia after CB2 activation with JWH015 (Ehrhart et al., 2005).

In addition, even though JWH015 increased the phagocytosis rate of A β (Ehrhart et al., 2005), our studies demonstrated that phagocytic uptake of A β by CB2^{-/-} microglia was similar to that of control microglia.

The results obtained with CB2 receptor deficient microglia indicated a modulatory role of this cannabinoid receptor in microglia activation. We therefore asked whether microglia functions are also changed in the absence of CB2 in an animal model expressing APP/

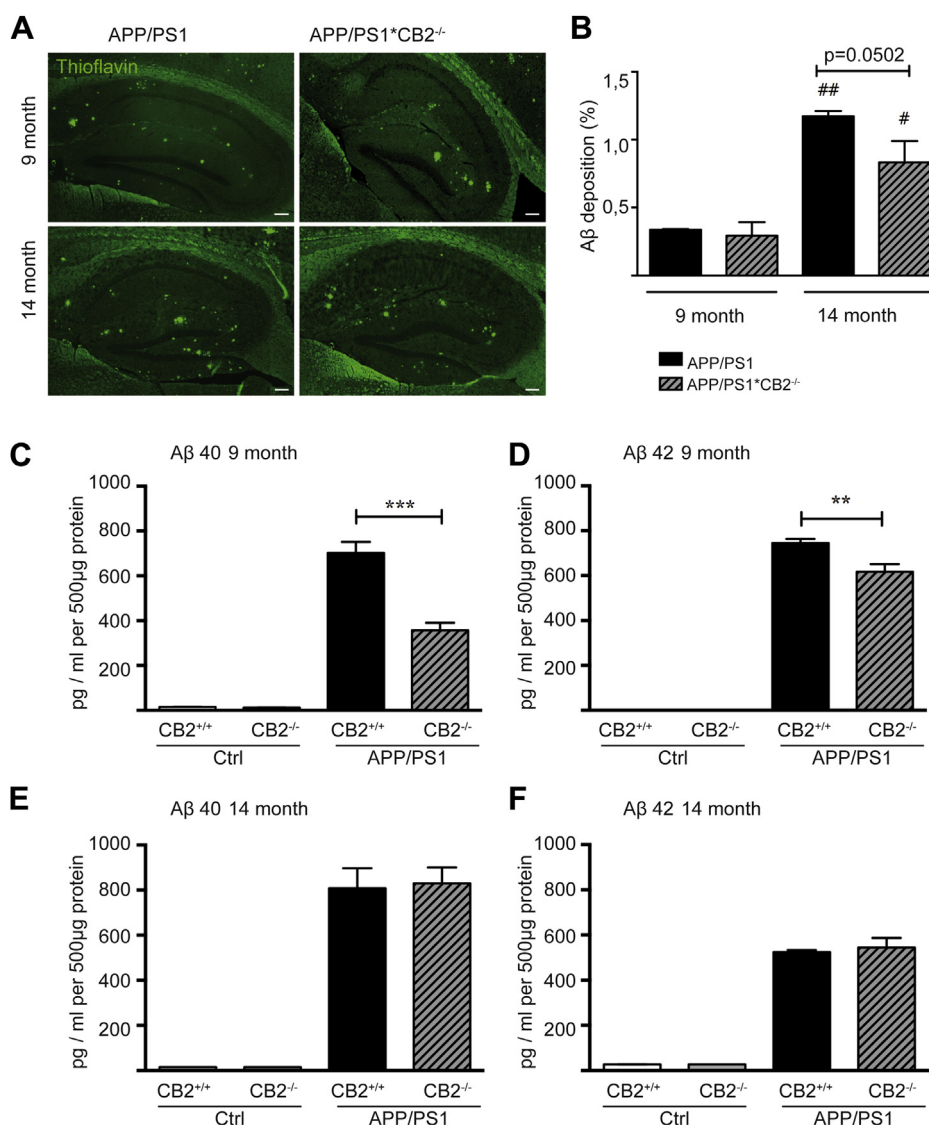


Fig. 6. Amyloid- β processing and plaque deposition in middle-aged and aged APP/PS1 and APP/PS1*CB2^{-/-} mice. (A) Representative immunohistological stainings of A β plaques stained with thioflavin S in sagittal brain slices of 9- and 14-month-old APP/PS1 and APP/PS1*CB2^{-/-} mice (scale bar = 200 μ m). (B) Quantitative analysis of amyloid- β depositions in the hippocampus of indicated groups of mice, ## $p < 0.01$; # $p < 0.05$: difference to 9-month-old genotype control; $n = 5$. (C–F) Quantitative analysis of amyloid- β 40 and 42 by enzyme-linked immunosorbent assay in brain lysates of 9- and 14-month-old mice. Reduced brain levels of A β 40 and A β 42 in 9-month-old APP/PS1*CB2^{-/-} mice compared to APP/PS1 controls (C and D). Differences in A β 40 and A β 42 were abrogated in 14-month-old mice (E and F); 2-way analysis of variance, followed by Fisher post hoc test. * $p < 0.05$, ** $p < 0.01$, *** $p < 0.001$. (For interpretation of the references to color in this Figure, the reader is referred to the web version of this article.)

PS1, which produces profound neuroinflammation. The degree of Iba-1 staining observed in the brains of APP/PS1*CB2^{-/-} mice suggested reduced microgliosis in the absence of CB2. This is in contrast to data presented by Koppel et al. (Koppel et al., 2013) that demonstrated enhanced levels of Iba1 staining in CB2^{-/-} mice using a different (J20 APP) genetic model of AD. Unfortunately, this study did not establish baseline Iba1 levels in CB2^{-/-} and CB2^{+/+} mice, data that would be of importance based on our observations that at baseline CB2^{-/-} mice presented increased levels of Iba1 staining.

To investigate whether increased levels of Iba1 immunoreactivity were due to an upregulation on respective cells or due to increased proliferation of Iba1⁺ cells, we also analyzed the degree of microgliosis and measured the percentages of infiltrating macrophages in aged APP/PS1 and APP/PS1*CB2^{-/-} mice by flow cytometry. APP/PS1*CB2^{-/-} mice showed a reduced percentage of microglia and infiltrating macrophages compared to APP/PS1 mice, suggesting that the number of cells immigrating in the CNS was reduced in the absence of CB2. In addition, microglia and

macrophages from APP/PS1*CB2^{-/-} mice expressed reduced levels of ICAM-1, an adhesion molecule involved in inflammatory responses. Consistent with this observation, we also found reduced expression levels of TNF α in APP/PS1 mice lacking CB2. It remains to be seen whether this reduction in ICAM-1 and TNF α production in the absence of CB2 is specific for the APP/PS1 transgenic mice, or whether it is also present in other neuroinflammation models. A recent study reported that treatment of APP/PS1 mice during the early symptomatic phase (at the age of 6 months) with a CB2 agonist reduced microglial-mediated pro-inflammatory responses (Aso et al., 2013). Neither CB2 deletion nor pharmacological stimulation of CB2 influenced the plaque load.

Nevertheless, pharmacological activation of CB2 improved cognition in APP/PS1 mice and treatment of APP/PS1 mice with JWH-133 during the pre-symptomatic (3 months of age) and early symptomatic (6 months of age) phases of AD had beneficial effects on learning and memory behavior as tested by the Y-Maze (Aso et al., 2013). In another study, in which A β -fibrils were injected

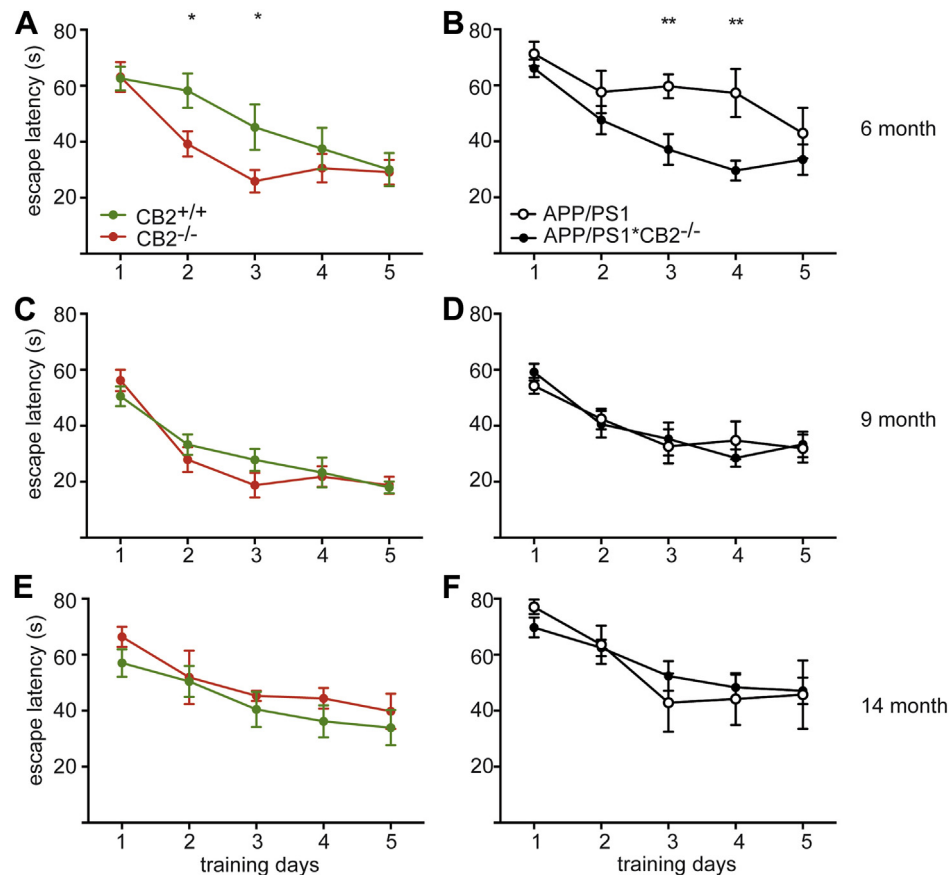


Fig. 7. Impaired cognitive performance in APP/PS1 and APP/PS1*CB2^{-/-} mice in Morris Water Maze test. Shown are learning curves of APP/PS1 (white circles), APP/PS1*CB2^{-/-} (black circles), WT (green), and CB2^{-/-} (red) mice at 6 (A and B), 9 (C and D), and 14 (E and F) months of age. The curves present average escape latencies (\pm SEM) to the hidden platform on each of 5 days of acquisition trials. Data analysis: significant differences were found in 6-month-old animals at days 2 and 3 in control animals and on days 3 and 4 in APP transgenic animals. No significant differences were found among the 4 different genotypes in the 9- and 14-month-old group. Data analysis: * $p < 0.05$ and ** $p < 0.01$, repeated measures 2-way analysis of variance and Fisher least squares difference (LSD) post hoc test ($n = 4$ –16 mice per group). (For interpretation of the references to color in this Figure, the reader is referred to the web version of this article.)

into rats, improved cognitive behavior was reported after CB2 agonist treatment (Wu et al., 2013). We observed beneficial effects of CB2 deletion on spatial learning and memory in 6-month-old AD and control mice in the Morris Water Maze test. However, this effect was no longer present at the age of 9 and 14 months. Thus, the CB2 deletion affects spatial learning during an early stage of the disease, but the reduction in neuroinflammation observed at a later stage does not seem to be sufficient to influence learning and memory performance in this test.

Since CB2-deficient neonatal microglia are already limited in their ability to respond to pro-inflammatory stimuli, it is likely, that CB2 at this juncture may affect immune system development. It seems possible that CCL2 plays a pivotal role during immune cell development, since CB2^{-/-} microglia released significantly reduced levels of CCL2 compared with CB2^{+/+} microglia. A similar observation was made in APP/PS1*CB2^{-/-} mice that expressed reduced levels of CCL2 compared to APP/PS1 mice. CCL2 is responsible for the recruitment of macrophages and microglia during CNS inflammation (Shi and Pamer, 2011), and the brains of CCL2-deficient APP/PS1 mice possessed fewer microglia (Kiyota et al., 2013). This suggests that the reduced microgliosis observed in APP/PS1*CB2^{-/-} mice could be due to reductions in CCL2 expression resulting in an impaired ability to recruit peripheral macrophages into the CNS. Taken together, our data demonstrated that deficiency of CB2 deletion affected both the recruitment of macrophages into the brains of AD mice and the ability to activate

microglia. Thus, CB2 receptors modulate specific aspects of the APP-induced neuropathology. Our findings warrant further investigation into the role of CB2 receptors as mediators of cannabinoid treatment effects in transgenic APP models.

Disclosure statement

The authors declare that they have no actual or potential conflicts of interest.

Acknowledgements

The authors thank Kerstin Michel and Andras Bilkei-Gorzo for assistance with MWM experiments. This work was supported by grants from the Deutsche Forschungsgemeinschaft (DFG) to J.A. (FOR926 SP10) and to A.Z. (FOR926 SP6, CP2). A.Z., P.N., D.B., and J.L.S. are members of the Excellence Cluster Immunosenescence.

References

- Aso, E., Juvés, S., Maldonado, R., Ferrer, I., 2013. CB2 cannabinoid receptor agonist ameliorates Alzheimer-like phenotype in A β PP/PS1 mice. *J. Alzheimers Dis.* 35, 847–858.
- Benito, C., Kim, W.K., Kim, W.K., Chavarría, I., Hillard, C.J., Mackie, K., Tolón, R.M., Williams, K., Romero, J., 2005. A glial endogenous cannabinoid system is upregulated in the brains of macaques with simian immunodeficiency virus-induced encephalitis. *J. Neurosci.* 25, 2530–2536.

- Benito, C., Tolo, R.M., Carrier, E.J., Ra, A., Hillard, C.J., 2003. Cannabinoid CB2 receptors and fatty acid amide hydrolase are selectively overexpressed in neuritic plaque-associated glia in Alzheimer's disease brains. *Neurology* 23, 11136–11141.
- Benito, C., Tolón, R.M., Pazos, M.R., Núñez, E., Castillo, A.I., Romero, J., 2008. Cannabinoid CB2 receptors in human brain inflammation. *Br. J. Pharmacol.* 153, 277–285.
- Bolmont, T., Haiss, F., Eicke, D., Radde, R., Mathis, C.A., Klunk, W.E., Kohsaka, S., Jucker, M., Calhoun, M.E., 2008. Dynamics of the microglial/amyloid interaction indicate a role in plaque maintenance. *J. Neurosci.* 28, 4283–4292.
- Buckley, N.E., McCoy, K.L., Mezey, E., Bonner, T., Zimmer, A., Felder, C.C., Glass, M., 2000. Immunomodulation by cannabinoids is absent in mice deficient for the cannabinoid CB(2) receptor. *Eur. J. Pharmacol.* 396, 141–149.
- Chen, R., Zhang, J., Fan, N., Teng, Z.Q., Wu, Y., Yang, H., Tang, Y.P., Sun, H., Song, Y., Chen, C., 2013. Δ^9 -THC-caused synaptic and memory impairments are mediated through COX-2 signaling. *Cell* 155, 1154–1165.
- Ehrhart, J., Obregon, D., Mori, T., Hou, H., Sun, N., Bai, Y., Klein, T., Fernandez, F., Tan, J., Shytle, R.D., 2005. Stimulation of cannabinoid receptor 2 (CB2) suppresses microglial activation. *J. Neuroinflammation* 2, 29.
- Gordon, M.N., King, D.L., Diamond, D.M., Jantzen, P.T., Boyett, K.V., Hope, C.E., Hatcher, J.M., DiCarlo, G., Gottschall, W.P., Morgan, D., Arendash, G.W., 2001. Correlation between cognitive deficits and Abeta deposits in transgenic APP+PS1 mice. *Neurobiol. Aging* 22, 377–385.
- Heneka, M.T., O'Banion, M.K., Terwel, D., Kummer, M.P., 2010. Neuroinflammatory processes in Alzheimer's disease. *J. Neural Transm.* 117, 919–947.
- Kiyota, T., Gendelman, H.E., Weir, R.A., Higgins, E.E., Zhang, G., Jain, M., 2013. CCL2 affects β -amyloidosis and progressive neurocognitive dysfunction in a mouse model of Alzheimer's disease. *Neurobiol. Aging* 34, 1060–1068.
- Koppel, J., Vingtdeux, V., Marambaud, P., d'Abramo, C., Jimenez, H., Stauber, M., Friedman, R., Davies, P., 2013. CB₂ receptor deficiency increases amyloid pathology and alters tau processing in a transgenic mouse model of Alzheimer's disease. *Mol. Med.* 19, 357–364.
- Lee, M.K., Borchelt, D.R., Kim, G., Thinakaran, G., Slunt, H.H., Ratovitski, T., Martin, L.J., Kittur, A., Gandy, S., Levey, A.I., Jenkins, N., Copeland, N., Price, D.L., Sisodia, S.S., 1997. Hyperaccumulation of FAD-linked presenilin 1 variants in vivo. *Nat. Med.* 3, 756–760.
- Martín-Moreno, A.M., Brera, B., Spuch, C., Carro, E., García-García, L., Delgado, M., Pozo, M.A., Innamorato, N.G., Cuadrado, A., de Ceballos, M.L., de Ceballos, M.L., 2012. Prolonged oral cannabinoid administration prevents neuroinflammation, lowers β -amyloid levels and improves cognitive performance in Tg APP 2576 mice. *J. Neuroinflamm.* 9, 8.
- Martín-Moreno, A.M., Reigada, D., Ramírez, G., Mechoulam, R., Innamorato, N., Cuadrado, A., de Ceballos, M.L., 2011. Cannabidiol and other cannabinoids reduce microglial activation in vitro and in vivo: relevance to Alzheimer's disease. *Mol. Pharmacol.* 79, 964–973.
- Michelucci, A., Heurtaux, T., Grandbarbe, L., Morga, E., Heuschling, P., 2009. Characterization of the microglial phenotype under specific pro-inflammatory and anti-inflammatory conditions: effects of oligomeric and fibrillar amyloid-beta. *J. Neuroimmunol.* 210, 3–12.
- Murray, P.J., Allen, J.E., Biswas, S.K., Fisher, E.A., Gilroy, D.W., Goerdt, S., Gordon, S., Hamilton, J.A., Ivashkiv, L.B., Lawrence, T., Locati, M., Mantovani, A., Martinez, F.O., Mege, J.-L., Mosser, D.M., Natoli, G., Saeji, J.P., Schultze, J.L., Shirey, K.A., Sica, A., Suttles, J., Udalova, I., van Ginderachter, J.A., Vogel, S.N., Wynn, T.A., 2014. Macrophage activation and polarization: nomenclature and experimental guidelines. *Immunity* 41, 14–20.
- Pacher, P., Mechoulam, R., 2011. Is lipid signaling through cannabinoid 2 receptors part of a protective system? *Prog. Lipid Res.* 50, 193–211.
- Ramírez, B.G., Blázquez, C., Gómez del Pulgar, T., Guzmán, M., de Ceballos, M.L., 2005. Prevention of Alzheimer's disease pathology by cannabinoids: neuroprotection mediated by blockade of microglial activation. *J. Neurosci.* 25, 1904–1913.
- Saura, J., Tusell, J.M., Serratos, J., 2003. High-yield isolation of murine microglia by mild trypsinization. *Glia* 44, 183–189.
- Shi, C., Pamer, E.G., 2011. Monocyte recruitment during infection and inflammation. *Nat. Rev. Immunol.* 11, 762–774.
- Wu, J., Bie, B., Yang, H., Xu, J.J., Brown, D.L., Naguib, M., 2013. Activation of the CB2 receptor system reverses amyloid-induced memory deficiency. *Neurobiol. Aging* 34, 791–804.